Cell

Endonucleolytic Function of MutLα in Human Mismatch Repair

Farid A. Kadyrov,[1] Leonid Dzantiev,[2] Nicoleta Constantin,[1] and Paul Modrich[1,2,*]
[1] Department of Biochemistry
[2] Howard Hughes Medical Institute
Box 3711, Duke University Medical Center, Durham, NC 27710, USA
*Contact: modrich@biochem.duke.edu
DOI 10.1016/j.cell.2006.05.039

SUMMARY

Half of hereditary nonpolyposis colon cancer kindreds harbor mutations that inactivate MutLα (MLH1•PMS2 heterodimer). MutLα is required for mismatch repair, but its function in this process is unclear. We show that human MutLα is a latent endonuclease that is activated in a mismatch-, MutSα-, RFC-, PCNA-, and ATP-dependent manner. Incision of a nicked mismatch-containing DNA heteroduplex by this four-protein system is strongly biased to the nicked strand. A mismatch-containing DNA segment spanned by two strand breaks is removed by the 5′-to-3′ activity of MutSα-activated exonuclease I. The probable endonuclease active site has been localized to a PMS2 $DQHA(X)_2E(X)_4E$ motif. This motif is conserved in eukaryotic PMS2 homologs and in MutL proteins from a number of bacterial species but is lacking in MutL proteins from bacteria that rely on d(GATC) methylation for strand discrimination in mismatch repair. Therefore, the mode of excision initiation may differ in these organisms.

INTRODUCTION

Inactivation of the human mismatch repair system increases the mutation rate several hundred-fold and is the primary cause of hereditary nonpolyposis colon cancer (HNPCC). Genetic stabilization afforded by this system has been attributed to its function in the correction of DNA biosynthetic errors, its role in ensuring the fidelity of genetic recombination, and its participation in the checkpoint and apoptotic responses to several classes of DNA damage (reviewed in Surtees et al., 2004; Stojic et al., 2004; Kunkel and Erie, 2005; Iyer et al., 2006). The reaction responsible for correction of replication errors is the best understood in molecular terms.

The mechanism of mismatch repair has been most extensively studied in *E. coli*, and the *E. coli* reaction has been reconstituted in a purified system (Kunkel and Erie, 2005; Iyer et al., 2006). Repair is directed to the daughter strand at the replication fork by virtue of the transient absence of d(GATC) methylation in newly synthesized DNA. Repair is initiated by binding of MutS to a mismatch, and MutL is recruited to the heteroduplex DNA in a MutS- and ATP-dependent manner. Assembly of the MutL•MutS•heteroduplex ternary complex is sufficient to activate the d(GATC) endonuclease activity of MutH, which incises the unmethylated strand. The ensuing strand break is the actual signal that directs repair to the new DNA strand and serves as an entry point for the excision system, comprised of DNA helicase II and an appropriate single-strand exonuclease. A 3′-to-5′ exonuclease is required when the MutH nick is introduced 3′ to the mismatch, while a 5′-to-3′ hydrolytic activity is necessary when the MutH strand break is 5′ to the mispair. DNA polymerase III holoenzyme repairs the ensuing gap, and ligase restores covalent integrity to the helix.

Mammalian cell extracts support a similar reaction in which repair is directed by a strand discontinuity (a nick or gap) that may also reside either 3′ or 5′ to the mismatch (Kunkel and Erie, 2005; Iyer et al., 2006). The key proteins for initiation of eukaryotic mismatch repair are homologs of bacterial MutS and MutL. Eukaryotes harbor two mismatch recognition activities, MutSα (MSH2•MSH6 heterodimer) and MutSβ (MSH2•MSH3 heterodimer), although MutSα is probably responsible for most mismatch repair events in mammalian cells. Eukaryotic MutL homologs also function as heterodimers, with MLH1 serving as a common subunit. The best characterized of these has been MutLα, isolated from both human (MLH1•PMS2 heterodimer) and yeast (MLH1•PMS1 complex) (Prolla et al., 1994; Li and Modrich, 1995; Habraken et al., 1998; Bowers et al., 2001; Raschle et al., 2002; Tomer et al., 2002).

Study of the mammalian extract reaction has implicated six activities in addition to MutSα, MutSβ, and MutLα in nick-directed mismatch repair: the PCNA replication clamp, the RFC clamp loader, the single-strand DNA binding protein RPA, exonuclease I (ExoI), DNA polymerase δ, and the DNA binding protein HMGB1 (Kunkel and Erie, 2005; Iyer et al., 2006). Surprisingly, ExoI, which

hydrolyzes duplex DNA with 5′-to-3′ polarity in the absence of other proteins, is required for both 5′- and 3′-directed repair of G-T or G-G mismatches in extracts of human and mouse cells (Genschel et al., 2002; Wei et al., 2003). However, extracts of an *ExoI*$^{-/-}$ mouse cell line retain significant activity on single-nucleotide and dinucleotide insertion/deletion heteroduplexes, and *HPRT* mutability of such cells is elevated 30-fold, substantially less than the 150-fold increase conferred by MSH2 deficiency (Wei et al., 2003). Although the spectrum of *HPRT* mutations was not established in the Wei et al. study, these findings indicate that ExoI plays a major role in the MutSα-dependent repair of base-base mispairs, but also that alternate excision activities may function in insertion/deletion mismatch correction.

These observations have led to several purified systems that support nick-directed mismatch-provoked excision and repair. The simplest of these consists of MutSα, MutLα, ExoI, and RPA (±HMGB1) (Genschel and Modrich, 2003; Zhang et al., 2005). Hydrolysis in this system is mismatch provoked but always proceeds 5′ to 3′ from the nick that directs excision. Although MutLα is not required in this system, it does enhance the mismatch dependence of the reaction by suppressing ExoI hydrolysis of mismatch-free DNA (Genschel and Modrich, 2003).

Supplementation of MutSα, MutLα, ExoI, and RPA with PCNA and RFC yields a system that supports bidirectional excision, i.e., excision directed by a nick located either 3′ or 5′ to the mismatch (Dzantiev et al., 2004). In contrast to the simpler 5′-to-3′ reaction, 3′-directed excision is absolutely dependent on MutLα, RFC, and PCNA. RFC apparently plays two roles in the activation of 3′-directed excision. It functions as a PCNA loader, with the loaded form of PCNA necessary to activate 3′-directed excision, but it also acts directly to suppress ExoI-mediated 5′-to-3′ hydrolysis from a nick or gap located 3′ to the mismatch (Dzantiev et al., 2004; N.C. and P.M., unpublished data). Since the activities other than ExoI used in this study were free of exonuclease activity and because an ExoI active-site mutant did not support 3′-directed excision, hydrolysis in this system was attributed to ExoI (Dzantiev et al., 2004). Addition of DNA polymerase δ to these six components yields a system that supports mismatch repair in a reaction that can be directed by a strand break located 3′ or 5′ to the mismatch (Constantin et al., 2005). As observed for 5′-directed excision, 5′-directed repair in this system is MutLα independent but requires RFC and PCNA for the repair synthesis step of the reaction.

The work described here clarifies the functions of MutLα and ExoI in human mismatch repair. We show that MutLα harbors a latent endonuclease that is activated in a mismatch-, MutSα-, RFC-, PCNA-, and ATP-dependent manner. Incision of a nicked heteroduplex by this four-protein system is strongly biased to the nicked strand. A mismatch-containing segment spanned by two strand breaks is then excised by the 5′-to-3′ action of MutSα-activated ExoI.

RESULTS

MutSα-, MutLα- RFC-, and PCNA-Dependent Endonucleolytic Cleavage of the Discontinuous Strand of a Nicked Heteroduplex

Biochemical analysis of human mismatch repair has relied on the use of circular substrates containing a mismatch and a strand discontinuity (a nick or a gap) that directs the reaction. Because mismatch-provoked excision in nuclear extracts is restricted to the shorter path linking the two DNA sites (Fang and Modrich, 1993), circular DNAs of this form are referred to as 3′ or 5′ heteroduplexes depending on whether the strand discontinuity resides 3′ or 5′ to the mispair, respectively, as viewed along the shorter path (see Figure 1 and Figure 2).

We have previously shown that a system comprised of MutSα, MutLα, RFC, PCNA, ExoI, and RPA supports 3′-nick-directed mismatch-provoked excision (Dzantiev et al., 2004). Subsequent experiments suggested that this reaction might involve MutSα-, MutLα-, RFC-, and PCNA-dependent endonucleolytic attack on the incised heteroduplex strand (data not shown). This was confirmed by Southern analysis after restriction endonuclease cleavage and resolution of DNA products on denaturing gels. The production of new DNA termini on a 3′ heteroduplex, as visualized by this method, is illustrated in Figure 1. Use of a radiolabeled probe complementary to the 3′ terminus of the nicked strand demonstrated the production of new DNA termini 5′ to the site of probe hybridization (Figure 1A). A mismatch, MutSα, MutLα, RFC, PCNA, and ATP were required for this effect, but RPA was not (lanes 1–7; see also Table S1 in the Supplemental Data available with this article online). Fifty percent of the products shown in Figure 1A range in size from 0.10 to 0.56 kb, although new termini as far as 3 kb from the original strand break were detectable (lanes 2 and 7). Because the nick-mismatch separation distance in this 3′ heteroduplex is 141 bp, these results imply that incision of this DNA occurred preferentially on the 5′ side of the mispair, although some incision 3′ to the mismatch also occurred. By contrast, the yield of these products was greatly reduced if ExoI was included in the reaction, as was the signal corresponding to the original heteroduplex 3′ terminus (Figure 1A, compare lane 8 with lanes 2 and 7).

The nature of endonucleolytic incision by this system was also addressed using probes that hybridize to the nicked heteroduplex strand on either side of the ClaI site (Figures 1B and 1C). The experiment shown in Figure 1B probes the other end of the DNA fragment analyzed in Figure 1A, i.e., for the production of new 3′ termini within this DNA segment. Incision products obtained in the presence of MutSα, MutLα, RFC, and PCNA (±RPA) and visualized with this probe were consistent with those observed in Figure 1A. As noted above, the occurrence of new 5′ termini within the region bracketed by the 3′ heteroduplex strand break and the ClaI site was abolished when ExoI was included in the reaction (Figure 1A, lane 8). However, generation of new 3′ termini within this region was

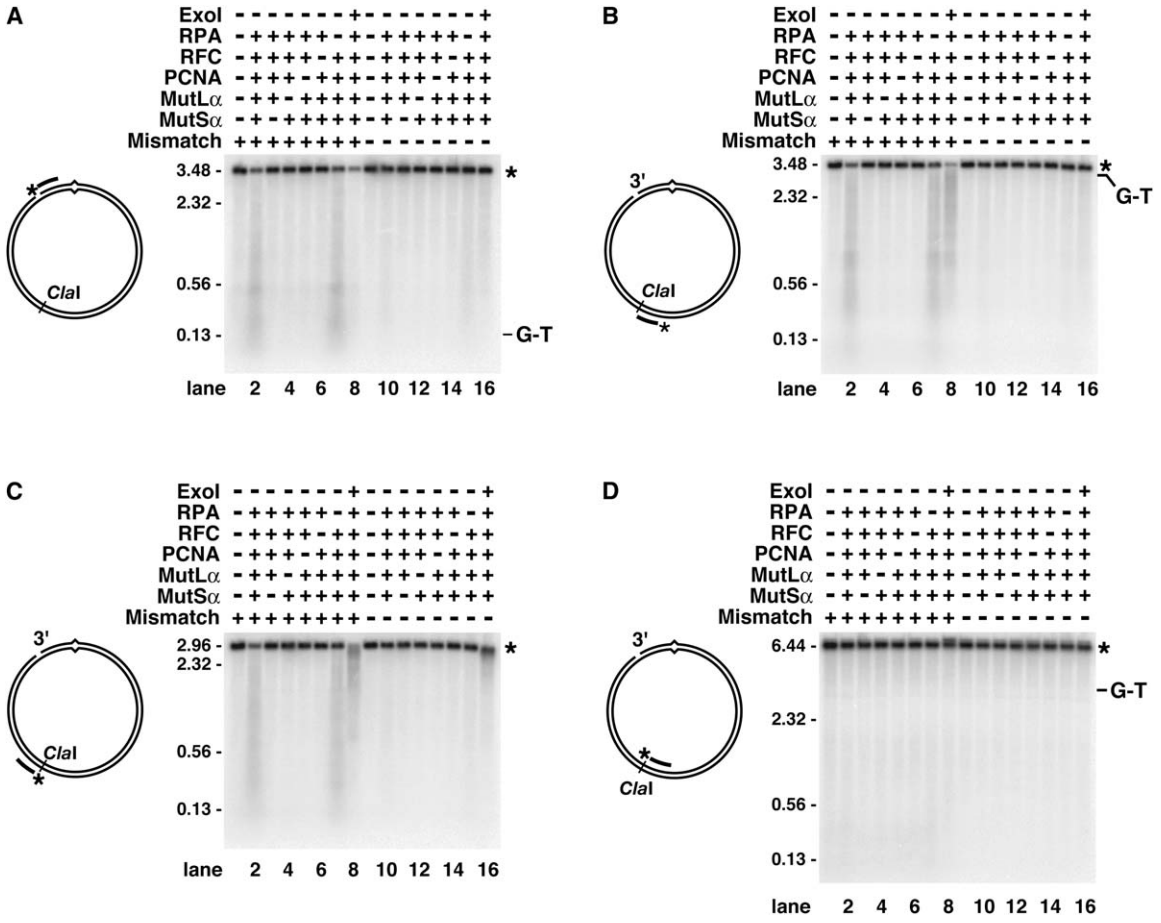

Figure 1. Incision of the Nicked Strand of a 3′ Heteroduplex by MutSα, MutLα, PCNA, and RFC

Reactions (see Experimental Procedures) contained nicked 3′ G-T heteroduplex or 3′ A•T homoduplex DNA and proteins as indicated. DNA products were cleaved with ClaI, resolved by electrophoresis through alkaline agarose gels, and transferred to nylon membranes (see Experimental Procedures), which were probed with ^{32}P-labeled oligonucleotides corresponding to f1MR59 (Dzantiev et al., 2004) viral strand coordinates 5491–5514 (A), viral strand coordinates 2505–2526 (B), viral strand coordinates 2531–2552 (C), or complementary strand coordinates 2505–2526 (D). When applicable, the location of the mismatch within the probed DNA fragment is indicated. The mobility of the full-length probed DNA segment is indicated by an asterisk; as described in the text, smaller DNA species are produced by endonuclease action.

demonstrable under these conditions (Figure 1B, lane 8). Because the MutSα, MutLα, RFC, PCNA, and RPA preparations used in these experiments were free of detectable exonuclease activity (Dzantiev et al., 2004; Table S1), the simplest explanation for these results is that 5′ termini produced by the endonucleolytic action of the MutSα, MutLα, RFC, PCNA system serve as entry sites for 5′-to-3′ hydrolysis by MutSα-activated ExoI (Genschel and Modrich, 2003; Dzantiev et al., 2004), which excises the DNA segment between this site and the original heteroduplex strand break, thus eliminating the hybridization target of the oligonucleotide probe.

Incubation of the 3′ heteroduplex with MutSα, MutLα, RFC, and PCNA (±RPA) also produced new termini on the 5′ side of the heteroduplex strand break (Figure 1C). However this effect was attenuated by ExoI, which led to the preferential elimination of those termini most distant from the mismatch (compare lane 8 with 2 and 7). A similar ExoI effect is evident in Figure 1B (lane 8 versus 2 and 7), and the products observed in the presence of ExoI in these two instances are similar to those observed previously in the defined 3′ excision system (Dzantiev et al., 2004). We think it unlikely that this preferential loss of distal termini is due to ExoI hydrolysis of hybridization target sequences in these cases. Rather, we attribute this effect to hydrolytic removal of the mismatch, which leads to *cis* inactivation of the endonucleolytic system. When inactivation in this manner does not occur, MutSα-, MutLα-, RFC-, and PCNA-dependent endonucleolytic incision is an ongoing process, and endonucleolytic events can occur several thousand bp from the mismatch. Additional evidence for this view is presented below.

Endonucleolytic attack on the nicked 3′ heteroduplex DNA by this system was strongly biased to the nicked strand; incision of the continuous strand was limited to about 10% of that occurring on the nicked strand

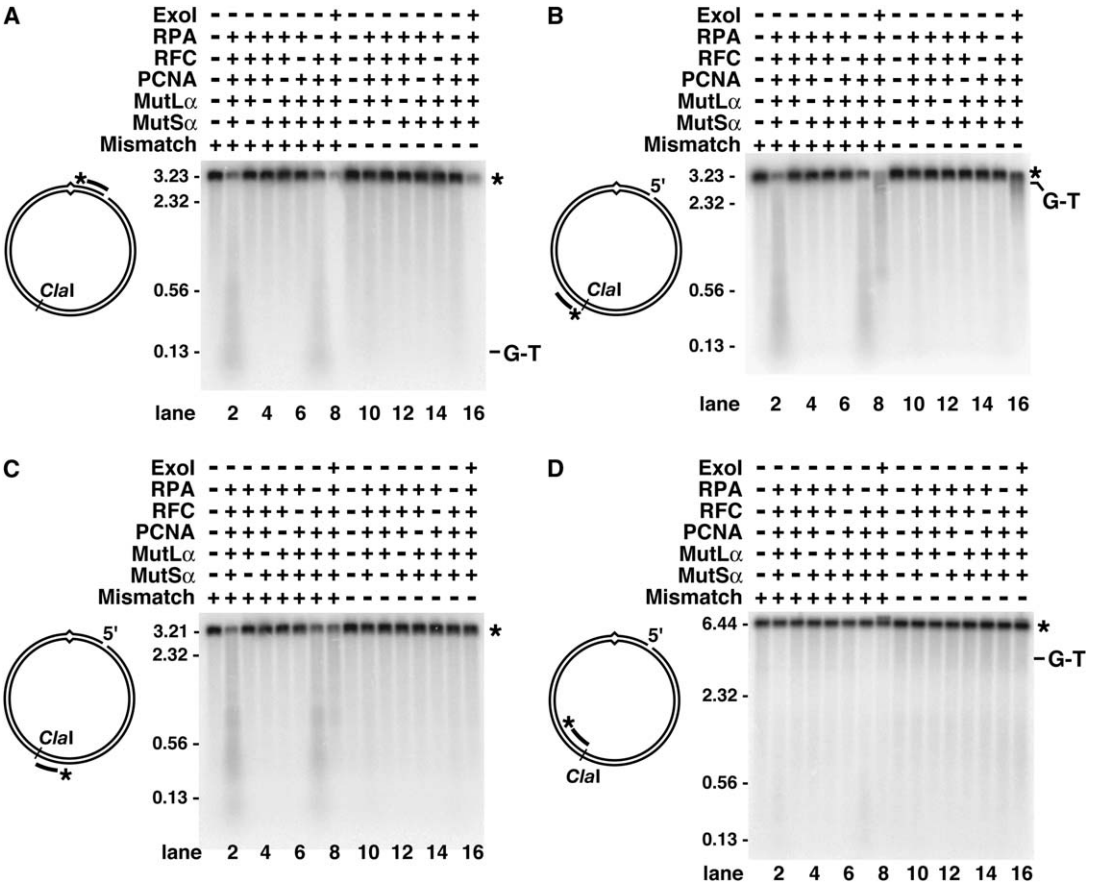

Figure 2. MutSα, MutLα, PCNA, and RFC Incise the Nicked Strand of 5′ Heteroduplex DNA

Reactions and analysis were as in Figure 1, except that substrates were nicked 5′ G-T heteroduplex or 5′ G•C homoduplex. DNA products were cleaved with ClaI, resolved by alkaline electrophoresis, and transferred to nylon membranes, which were probed with ^{32}P-labeled oligonucleotides corresponding to f1MR1 (Su et al., 1988) viral strand coordinates 5732–5755 (A), viral strand coordinates 2531–2552 (B), viral strand coordinates 2505–2526 (C), or complementary strand coordinates 2531–2552 (D).

(Figure 1D; Table S1; see also below). Furthermore, covalently closed circular heteroduplex and homoduplex DNAs were resistant to incision by this system (Figure S1).

The nicked strand of a 5′ G-T heteroduplex (nick and mismatch separated by 128 bp) was also subjected to incision in the presence of MutSα, MutLα, RFC, and PCNA (Figure 2). As observed with 3′ substrates, incision was mismatch dependent and occurred in the absence of RPA (Figures 2A–2C), and the continuous heteroduplex strand was resistant (incision was about 6% of that occurring on the nicked strand; compare Figure 2D with Figures 2A–2C; Table S1). Furthermore, supplementation of these proteins with ExoI abolished endonucleolytic product signals when the oligonucleotide used for end labeling was complementary to 5′ terminus at the nick that directs the reaction (Figure 2A, compare lane 8 with lanes 2 and 7). Presence of the exonuclease also attenuated incision events occurring in the vicinity of the ClaI site distal from the mismatch (Figures 2B and 2C, compare lane 8 with lanes 2 and 7). Table S1 quantifies the results of the incision reactions presented in Figure 1 and Figure 2. As can be seen, 5′ and 3′ heteroduplexes are incised with similar efficiency and in a manner that is highly dependent on a mismatch, MutSα, MutLα, RFC, PCNA, and ATP.

5′-to-3′ ExoI Hydrolysis Removes a DNA Segment Spanning the Mismatch in a 3′ Heteroduplex

We have previously shown that MutSα, MutLα, ExoI, RFC, PCNA, and RPA are sufficient to support ATP-dependent excision directed by a strand break located 3′ to a mismatch. The experiments described above suggested that the endonucleolytic products produced in the presence of MutSα, MutLα, RFC, and PCNA are intermediates in this process. Indeed, the MutSα and MutLα dependence of the endonucleolytic reaction is similar to that of reconstituted 3′-directed excision (Figure S2), and homogeneous yeast RFC effectively substituted for human RFC in this system (Table S1), as it does in 3′-directed excision (Dzantiev et al., 2004). Additional evidence for endonucleolytic involvement in 3′-directed excision was provided by the experiment shown in Figure 3A, which used an oligonucleotide probe complementary to that portion of

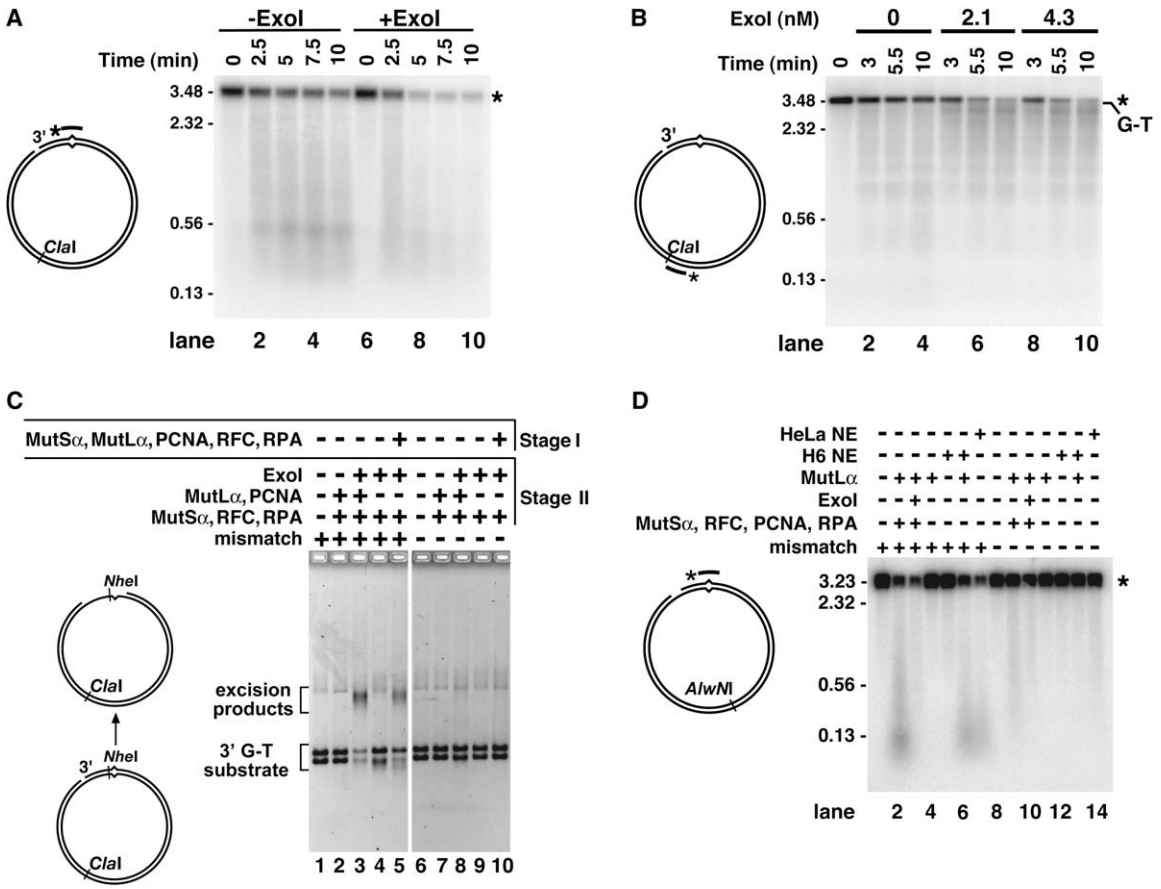

Figure 3. The Intermediate Produced by Incision of a 3′ Heteroduplex Is Degraded by ExoI and Occurs in Nuclear Extracts

(A) Nicked 3′ G-T heteroduplex was incubated with MutSα, MutLα, RFC, and PCNA in the absence or presence of 2.1 nM ExoI as described in Experimental Procedures, except that reaction time was varied as shown. Products were cleaved with ClaI, resolved by alkaline agarose gel electrophoresis, transferred to nylon membranes as in Figure 1, and probed with a ^{32}P-labeled oligonucleotide corresponding to f1MR59 viral strand coordinates 5629–5652.

(B) Dependence of the kinetics and locations of 5′ termini production as a function of ExoI concentration was determined as described in (A), except that reactions were sampled as a function of time and ExoI was present as indicated. Products were probed with a ^{32}P-labeled oligonucleotide corresponding to f1MR59 viral strand coordinates 2505–2526.

(C) Reactions containing nicked 3′ G-T heteroduplex or A•T homoduplex DNA and proteins as shown were performed as described in Experimental Procedures, except that incubations were carried in two stages. Stage I reactions were performed in the absence or presence of MutSα, MutLα, RFC, PCNA, and RPA as indicated. After deproteinization with Proteinase K and phenol/chloroform extraction, recovered DNA was employed as substrate in a stage II incubation in the presence of the indicated proteins. Mismatch-provoked excision was scored by cleavage with NheI and ClaI followed by electrophoresis on native agarose gels (Genschel et al., 2002). As illustrated in the diagram on the left, excision renders the DNA resistant to NheI cleavage, the recognition site for which is located 5 bp from the mismatch.

(D) Reactions (see Experimental Procedures) contained gapped 3′ A-C heteroduplex or A•T homoduplex, nuclear extract (NE), and/or proteins as indicated. The distance between the 150 nucleotide gap and the mismatch was 51 nucleotides as viewed along the shorter path in the circular substrate. DNA products were cleaved with AlwNI, resolved on an alkaline agarose gel, and transferred to nylon membranes (Figure 1), which were probed with ^{32}P-labeled oligonucleotides corresponding to M13B276 viral strand coordinates 6541–6564. Location of the full-length probed segment is indicated.

the nicked heteroduplex strand spanning the mismatch. As can be seen, endonucleolytic products containing the mismatched base appeared and disappeared when ExoI was included in the reaction, as expected for a reaction intermediate (compare lanes 2–5 with lanes 7–10). Results of this kinetic analysis were also consistent with the above suggestion that hydrolytic removal of the mismatch inactivates the endonuclease system in *cis* to prevent incision events from occurring at sites distal from the mispair. As can be seen in Figure 3B, incision in the vicinity of the ClaI site was also suppressed when the endonucleolytic system was supplemented with ExoI.

Whereas MutSα, ExoI, and RPA are sufficient for excision of a mismatch when the nick that directs hydrolysis is located 5′ to the mispair (Genschel and Modrich, 2003; Zhang et al., 2005), mismatch excision directed by a 3′ strand break additionally requires MutLα, RFC, and PCNA (Dzantiev et al., 2004). Figure 3C demonstrates

that the activity requirements for 3′-directed excision can be resolved in a two-stage reaction. Mismatch removal from the 3′ heteroduplex occurred in a stage 2 incubation lacking MutLα and PCNA provided that the heteroduplex was previously incubated with MutSα, MutLα, RFC, PCNA, and RPA, components sufficient for endonucleolytic incision of the DNA (lanes 1–5). Because MutSα, RPA, and a mismatch are sufficient to activate 5′-to-3′ hydrolysis by ExoI (Genschel and Modrich, 2003), we attribute 3′-directed excision in this system to the 5′-to-3′ hydrolytic function of ExoI initiating at a strand break introduced on the 5′ side of the mispair by the action of MutSα, MutLα, RFC, and PCNA.

Mismatch-dependent production of endonucleolytic intermediates can also be detected in nuclear extracts of human cells. In order to reduce heteroduplex ligation in extracts, these experiments employed a circular A-C heteroduplex (or A•T homoduplex) containing a 150 nucleotide gap located 51 bp 3′ to the mismatch (Figure 3D). The gapped heteroduplex supported mismatch-dependent endonuclease in the presence of MutSα, MutLα, RFC, and PCNA (Figure 3D, compare lanes 2 and 9). DNA fragments spanning the mismatch were also produced in HeLa nuclear extracts, and production of this species was also mismatch dependent (lanes 7 and 14). By contrast, fragments spanning the mispair were not produced in extracts derived from *MLH1*$^{-/-}$ H6 tumor cells, although supplementation of H6 extract with near homogeneous MutLα led to production of this species in a manner similar to that observed in HeLa extracts (lanes 5–7). As in the purified system, DNA fragments produced in nuclear extracts were derived from the discontinuous heteroduplex strand (Figure S3A). However, heteroduplex incision in nuclear extracts was more restricted to the vicinity of the mismatch than endonucleolytic events occurring in the purified system were (Figure S3B, lane 2 versus lanes 6 and 7). A similar effect has been noted previously with respect to termini produced in the MutSα-, MutLα-, ExoI-, RFC-, PCNA-, and RPA-dependent 3′-directed excision system (Dzantiev et al., 2004). These purified systems thus lack one or more activities that function to restrict action of the endonuclease component to the vicinity of the mispair.

MutLα Is a Latent Endonuclease that Is Activated by RFC, PCNA, and MutSα

Two completely independent sets of near homogeneous proteins were used in this work, and individual preparations were free of detectable nonspecific endonuclease activity in presence of ATP and Mg^{2+} at the salt concentration used for mismatch repair assay (125 mM KCl) (Figure 1, Figure 2, and Figure S2). However, MutSα, MutLα, RFC, or PCNA must harbor the active site of the endonuclease observed in this system. Studies in our and other laboratories have failed to reveal such an activity associated with PCNA or RFC, and we have been unable to detect endonuclease activity in MutSα preparations. However, we have found that MutLα preparations display endonuclease activity under certain conditions. A weak endonuclease activity that incises closed circular supercoiled homoduplex DNA was detectable at low KCl concentration (23 mM) in the presence of 1 mM Mn^{2+} but was not detectable in the presence of Mg^{2+} (Figures 4A and 4B). The Mn^{2+}-dependent activity was stimulated by 0.5 mM ATP (Figure 4A, compare lanes 2 and 3), consistent with the known involvement of MutLα ATP hydrolytic centers in mismatch repair (Tomer et al., 2002; Raschle et al., 2002), and was further activated by RFC and PCNA, an effect dependent on the presence of both proteins (Figure 4C). Mn^{2+}-dependent incision of supercoiled circular DNA was independent of the presence of a mismatch within the molecule (compare Figures 4C and 4D).

While this putative MutLα endonuclease displays a RFC and PCNA dependence similar to that of the mismatch-provoked reaction described above, it is nevertheless a weak activity. For this reason, association of this activity with MutLα was evaluated by cofractionation. Homogeneous recombinant MutLα was subjected to an additional chromatography step on phosphocellulose, which was not used during isolation of the protein. Endonuclease activity determined in the presence of ATP•Mn^{2+} coeluted from the resin with the MLH1•PMS2 heterodimer (Figure S4A), and similar results were obtained upon gel filtration through Superdex 200 (Figure S4B). Figure S4C illustrates the seventh column step during isolation of MutLα from HeLa nuclear extracts. As can be seen, ATP•Mn^{2+}-dependent endonuclease activity, which is activated in the presence of MutSα, RFC, and PCNA, cochromatographs on MonoS with HeLa MutLα, which was scored by Western blot for the PMS2 subunit and by its ability to complement nuclear extract of *MLH1*$^{-/-}$ tumor cells to restore mismatch-provoked excision.

Immunological analysis also indicated tight association of ATP•Mn^{2+}-dependent endonuclease with MutLα. As shown in Figure S4D, incubation of near homogeneous MutLα with a Protein A-linked anti-PMS2 peptide antibody followed by removal of Protein A beads resulted in a comparable depletion of MutLα polypeptides and ATP•Mn^{2+}-dependent endonuclease activity.

A Metal Binding Site near the PMS2 C Terminus Is Required for MutLα Endonuclease

Because endonucleolytic hydrolysis depends on one or two divalent cations (Galburt and Stoddard, 2002), Fe^{2+}-dependent hydroxyl radical cleavage (Zaychikov et al., 1996) was employed to locate metal binding sites within MutLα. Incubation of MutLα with Fe^{2+} and a reducing agent in the absence of ATP revealed a major cleavage site, which maps near the C terminus of the PMS2 subunit between methionines 672 and 711, but closer to the latter residue (Figures 5A–5D). A BLAST screen of the sequence bracketed by these two residues against the protein database revealed a DQHA$(X)_2$E$(X)_4$E motif that is highly conserved in eukaryotic homologs of human PMS2 and MLH3 and is also found in archaeal and eubacterial MutL proteins but is lacking in MLH1 and MutL proteins

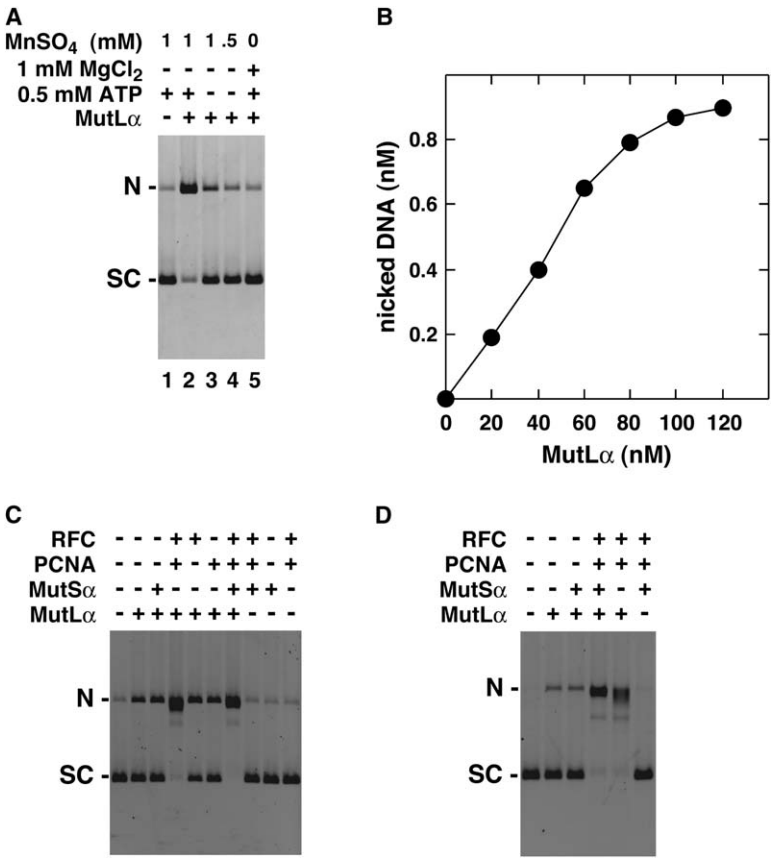

Figure 4. Recombinant MutLα Displays Mn^{2+}-Dependent Endonuclease Activity that is stimulated by RFC, PCNA, and ATP

(A) Endonuclease activity on supercoiled homoduplex f1MR59 DNA was determined as described in Experimental Procedures, except that ATP, $MnSO_4$, and $MgCl_2$ were varied as shown. When present, MutLα concentration was 80 nM.

(B) Endonuclease activity on supercoiled f1MR59 DNA in the presence of ATP-Mn^{2+} (see Experimental Procedures) was determined as a function of MutLα concentration in the absence of other proteins.

(C and D) ATP-Mn^{2+} endonuclease reactions (see Experimental Procedures) contained MutSα, MutLα, RFC, and PCNA as indicated and supercoiled homoduplex f1MR59 DNA (C) or supercoiled G-T heteroduplex DNA (D).

from bacteria that rely on d(GATC) methylation to direct mismatch repair (Figure 5E).

To assess the significance of this metal binding motif, we constructed MutLα variants with PMS2 D699N or E705K amino acid substitutions. The latter mutation has been identified in a Turcot's syndrome kindred (Miyaki et al., 1997), although a causative link between the mutation and the disease was not established. MLH1•$PMS2_{D699N}$ (MutLαD699N) and MLH1•$PMS2_{E705K}$ (MutLαE705K) were expressed in SF9 insect cells using baculovirus vectors. MutLαD699N and MutLαE705K, which were isolated in near homogeneous form as 1:1 heterodimers (Figure S5), fractionated like wild-type protein (data not shown), displayed normal ATP hydrolytic activity, and supported mismatch-dependent assembly of the MutLα•MutSα• heteroduplex ternary complex (Figure S6). However, Fe^{2+} binding to the C-terminal PMS2 motif was abolished in both mutant proteins as judged by hydroxyl radical cleavage (Figure 5F). Both mutant proteins were also defective in ATP-Mn^{2+}-dependent endonuclease activity; failed to support mismatch repair upon supplementation of MutLα-deficient nuclear extract prepared from H6 cells; and were inactive in the MutSα-, MutLα-, RFC-, and PCNA-dependent incision of the nicked strand of a G-T heteroduplex (Figure 6). The simplest explanation for these findings is that the PMS2 DQHA$(X)_2$E$(X)_4$E motif represents a part of the MutLα endonuclease active site.

MutSα-, MutLα-, RFC-, and PCNA-Dependent Incision of a Nicked Heteroduplex Requires Integrity of the MutLα ATP Hydrolytic Centers

As described above, ATP is required for MutSα-, MutLα-, RFC-, and PCNA-dependent incision of a nicked heteroduplex and also enhances Mn^{2+}-dependent MutLα endonuclease activity. A MutLα variant that harbors amino acid substitutions for MLH1 Glu-34 and PMS2 Glu-41 within the ATPase centers binds ATP but is largely defective in mismatch repair (Tomer et al., 2002; Raschle et al., 2002). As shown in Figure S7A, MLH1_{E34A}•His_6-$PMS2_{E41A}$ (His-MutLαEA) also fails to support 3′-directed mismatch-provoked excision in the purified system and in nuclear extracts. The mutant protein is also defective in its ability to support endonucleolytic cleavage of the nicked strand of heteroduplex DNA in the presence of MutSα, PCNA, RFC, RPA, and ATP (Figure S7B). Thus, in addition to the C-terminal metal binding site, integrity of MutLα ATPase centers is required for its ability to support incision of a nicked heteroduplex in this four-component system.

DISCUSSION

Human MutLα was initially isolated by virtue of its ability to restore mismatch repair to nuclear extracts of genetically unstable colon tumor cells (Li and Modrich, 1995). Despite its importance in mismatch repair and the fact that roughly

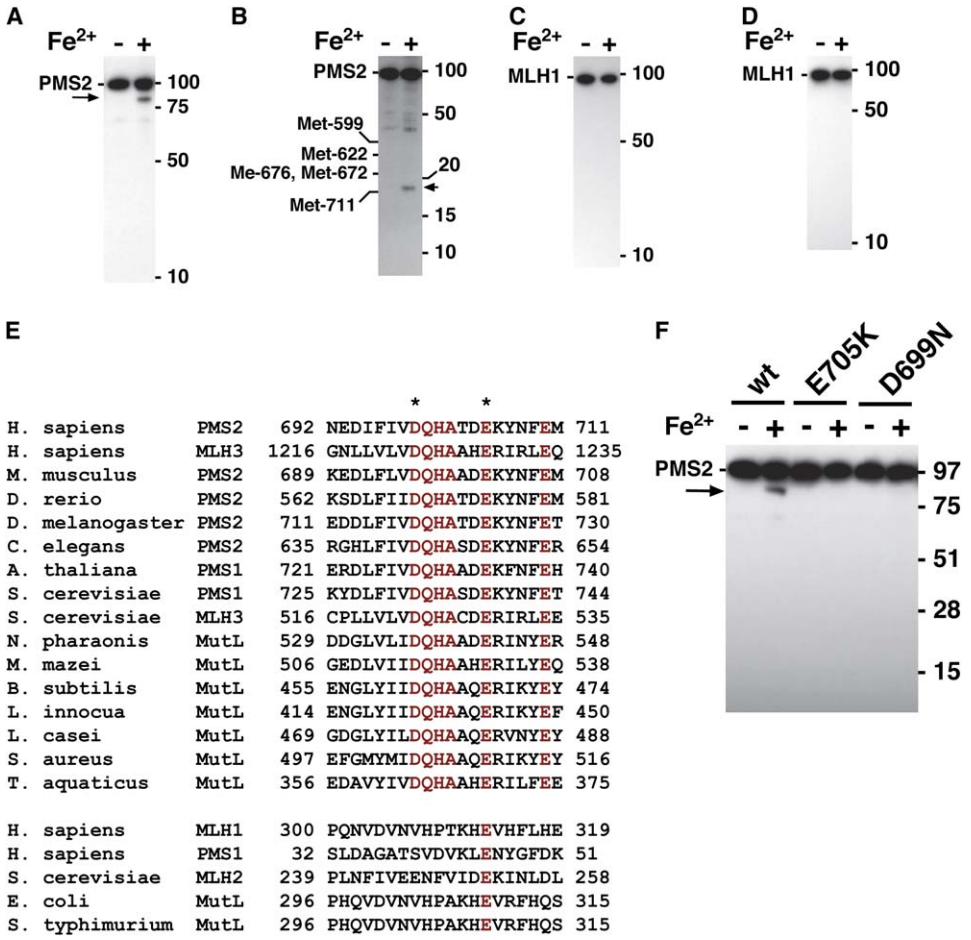

Figure 5. MutLα Contains a Metal Binding Site in the C-Terminal Portion of PMS2

(A–D) MutLα was incubated in the absence or presence of 20 μM Fe^{2+} as indicated (see Experimental Procedures). Products were separated on 4%–12% SDS (A and D) or 12% SDS (B and C) gels and visualized by Western blot using α-PMS2 directed against amino acids 9–54 (A), α-PMS2 directed against residues 800–862 (B), α-MLH1 directed against amino acids 633–662 (C), or α-MLH1 directed against the full-length MLH1 polypeptide (D). Arrows indicate the major PMS2 product resulting from radical cleavage. Location of PMS2 peptides produced by single-hit cyanogen bromide cleavage (Grachev et al., 1989) at PMS2 methionine residues 599, 622, 672, 676, and 711 are shown in (B).

(E) Human PMS2 residues located between Met-676 and Met-711 were employed for homology search using the BLAST routine available at http://www.ncbi.nlm.nih.gov/blast. Alignments shown for the five sequences at the bottom were obtained by running the human PMS2 DQHATDEKYNFE motif against indicated polypeptide sequences using MegAlign (DNAStar). Conserved residues are shown in red. Asterisks indicate human PMS2 residues altered in this study.

(F) Wild-type MutLα, MutLαE705K, and MutLαD699N were subjected to Fe^{2+}-dependent hydroxyl radical cleavage and analyzed as described in (A). Controls were incubated in the absence of Fe^{2+} as indicated.

half of HNPCC mutations lead to MutLα alterations (Peltomaki, 2005), the only information available on the function of the protein was the fact that it is recruited to heteroduplex DNA in a MutSα- and ATP-dependent fashion (Habraken et al., 1998; Blackwell et al., 2001). The demonstration that MutLα is a latent endonuclease, activated in a mismatch-, MutSα-, RFC-, and PCNA-dependent manner, provides a novel context in which to view its function in mismatch repair. We have also found that MutLα displays an ATP-Mn^{2+}-dependent endonuclease activity that can be detected on homoduplex DNA at low salt concentration. We think it unlikely that the latter activity has biological significance because a Mn^{2+} concentration corresponding to the intracellular level (35 μM; Ash and Schramm, 1982) is not sufficient to support the reaction (data not shown).

These findings are of interest in view of the requirement for ExoI in 3′-directed excision both in nuclear extracts (Genschel et al., 2002; Wei et al., 2003) and in a purified system comprised of MutSα, MutLα, RFC, PCNA, RPA, and ExoI (Dzantiev et al., 2004). Because ExoI hydrolyzes duplex DNA with 5′-to-3′ polarity (Lee et al., 2002), the question has been the identity of the activity responsible for 3′-directed hydrolysis. The findings described here obviate the requirement for a 3′-to-5′ hydrolytic activity in this defined system. As illustrated in Figure 7, incision of a 3′

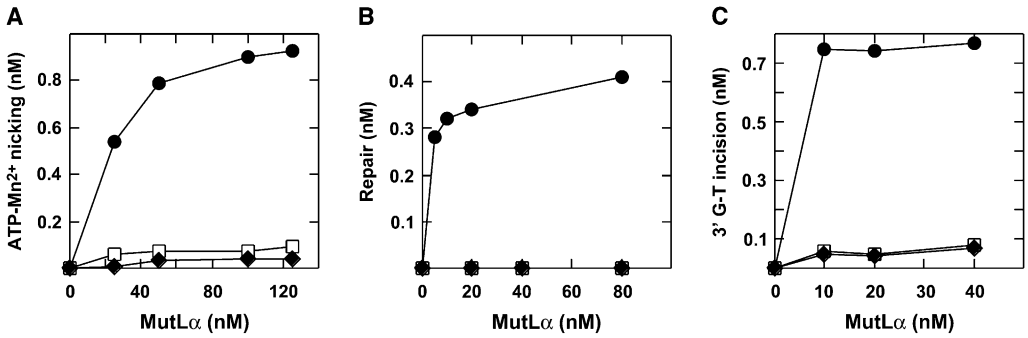

Figure 6. MutLαE705K and MutLαD699N Are Defective in Both Endonuclease and Mismatch Repair Activities

Wild-type MutLα (●), MutLαE705K (□), and MutLαD699N (◆) were analyzed for activities as follows.

(A) ATP•Mn^{2+}-dependent endonuclease activity in the absence of other proteins was determined as described in Experimental Procedures, except that 23 mM NaCl was substituted for 23 mM KCl.

(B) The three proteins were scored for their ability to restore mismatch repair to nuclear extracts of *MLH1*$^{-/-}$ H6 cells.

(C) Incision of nicked 3′ G-T heteroduplex DNA was determined in the presence of MutSα, RFC, PCNA, RPA, ATP-Mg^{2+}, and wild-type or mutant MutLα as indicated. Reactions and analysis were as in Figure 1B. Results were quantitated by PhosphorImager analysis.

heteroduplex by MutSα, MutLα, RFC, and PCNA, which tends to occur on the distal side of the mispair relative to the nick that directs the reaction, provides a 5′ terminus that can serve as an entry site for 5′-to-3′ hydrolysis by MutSα-activated ExoI (Genschel and Modrich, 2003). This accounts for the ability of MutSα, MutLα, ExoI, RFC, PCNA, and RPA to support 3′-directed excision. It is also noteworthy that although MutLα, RFC, and PCNA are dispensable for excision directed by a 5′ strand break (Genschel and Modrich, 2003), 5′ heteroduplexes are nevertheless subject to incision by the MutSα, MutLα, RFC, PCNA system. Hence, at least two distinct pathways exist that are capable of supporting 5′-directed mismatch-provoked excision.

This study also clarifies differences between the findings of Zhang et al. (2005) and those described by Dzantiev et al. (2004) and Constantin et al. (2005). Zhang et al. have described reconstituted 5′-directed mismatch repair in a system comprised of MutSα, MutLα, ExoI, RPA, and DNA polymerase δ. RPA can be replaced in this system by HMGB1, and MutLα is dispensable for the 5′-directed reaction as it is in the system described above. However, this system differs significantly from those described by Dzantiev et al. and Constantin et al. Reconstituted 5′-directed repair in the system of Zhang et al. is independent of RFC and PCNA and requires a much higher DNA polymerase δ concentration than that described by Constantin et al. Furthermore, in contrast to the findings of Dzantiev et al. and Constantin et al., it does not support 3′-directed excision or repair when RFC and PCNA are present. One explanation for the differences between the findings of Dzantiev et al. and Zhang et al. is suggested by the fact that the p38 subunit was dramatically underrepresented in the recombinant RFC preparation used by Zhang et al. (see Supplemental Data in Zhang et al., 2005). Reduced RFC activity would explain the failure of Zhang et al. to observe the expected dependence of 5′-directed repair on PCNA, which is known to be required for the repair synthesis step of the reaction (Gu et al., 1998; Genschel and Modrich, 2003; Guo et al., 2004). It would also account for the high polymerase δ concentration necessary in their experiments, as well as their inability to detect 3′-directed excision and repair.

Although incision by the MutSα, MutLα, RFC, PCNA system is strongly biased (10- to 20-fold) to the discontinuous strand of a nicked circular heteroduplex, low but detectable incision of the continuous heteroduplex strand does occur (Figure 1; Figure 2; Table S1). This strong but not absolute strand bias could be an intrinsic feature of the human mismatch repair system. However, low-level incision of the continuous strand could also reflect limitations of our purified system, e.g., failure to reproduce the in vivo ionic environment and/or deficiency of one or more activities that modulate MutLα activation.

Endonucleolytic action of this system is directed by a preexisting nick or gap, but incision occurs elsewhere on the helix. The strand bias characteristic of this reaction implies that the system is capable of maintaining the identity of the discontinuous heteroduplex strand over a substantial distance along the DNA contour. This effect is formally analogous to the ability of the *E. coli* mismatch repair system to establish heteroduplex orientation and requires signaling along the helix. Although the mechanism of signaling during mismatch repair is the subject of active debate, a favored model invokes ATP-promoted movement of MutSα and the MutSα•MutLα complex along the helix contour (Kunkel and Erie, 2005; Iyer et al., 2006).

The molecular roles of RFC and PCNA in the activation of MutLα endonuclease also remain to be defined. However, because RFC loading of PCNA onto the helix is necessary for 3′-directed excision (Dzantiev et al., 2004), it seems probable that the loaded form of PCNA will prove necessary for endonuclease activation. MutLα-MutSα, MutSα-PCNA, and MutLα-PCNA interactions have been

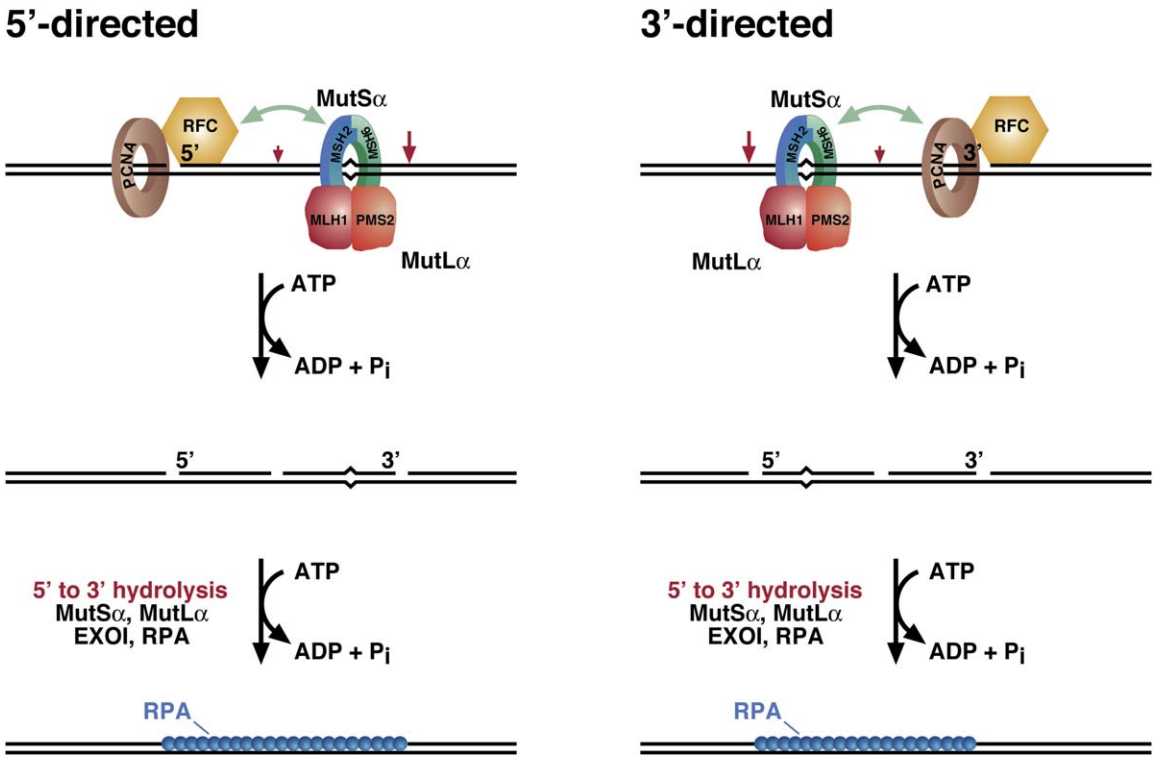

Figure 7. Incision of the Discontinuous Heteroduplex Strand in Human Mismatch Repair

The model shown summarizes observations of this study. MutSα, PCNA, and RFC activate a latent MutLα endonuclease, which incises the discontinuous strand of 5′ or 3′ heteroduplex DNAs in an ATP-dependent reaction. For the substrates tested here, incision displays a bias for occurrence on the distal side of the mismatch relative to the location of the original strand break (large red arrows) but can also occur proximal to the mispair (small red arrows). For a 3′ heteroduplex, this yields a new 5′ terminus on the distal side of the mismatch that serves as an entry site for MutSα-activated ExoI, which removes the mismatch in a 5′-to-3′ hydrolytic reaction controlled by RPA (Genschel and Modrich, 2003). As described in the Discussion, the strong bias for incision of the discontinuous strand implies signaling along the helix contour, which may involve ATP-promoted movement of MutSα or the MutSα•MutLα complex along the helix. This feature of the mechanism is not illustrated in the diagram shown.

documented (Dzantiev et al., 2004; Kunkel and Erie, 2005; Iyer et al., 2006; Lee and Alani, 2006), and it would not be surprising if PCNA interaction with MutLα, MutSα, or both proteins were to play a key role in MutLα activation.

Because optimal conditions for mismatch repair in both extracts and purified systems involve a substantial molar excess of MutLα over heteroduplex (Dzantiev et al., 2004; Zhang et al., 2005; Constantin et al., 2005), a valid k_{cat} for the activated form of MutLα endonuclease cannot be calculated. A minimum value for this parameter of 0.03 min^{-1} can be estimated from the data in Figure S2, but the actual value may be considerably higher. Nevertheless, this minimum estimate compares favorably with the value of 0.1 min^{-1} determined for the *E. coli* MutH endonuclease upon activation by MutS and MutL (Au et al., 1992).

We have also detected occurrence of an incised heteroduplex intermediate in human cell nuclear extracts that is similar to that produced in the MutSα, MutLα, RFC, PCNA system. Production of this species in nuclear extracts is mismatch and MutLα dependent, suggesting that it is a bona fide intermediate in mismatch repair. However, the reaction that produces this intermediate in the purified system differs somewhat from that in nuclear extracts. Incision events in nuclear extracts are more restricted to the vicinity of the mispair than those that occur in the purified system are (Figure S3A). A related effect has been previously noted with respect to excision tract length in the bidirectional excision system comprised of MutSα, MutLα, ExoI, RFC, PCNA, and RPA (Dzantiev et al., 2004). These observations imply that the four-component endonucleolytic system and the six-component excision system are lacking one or more regulatory activities that modulate their DNA hydrolytic functions. We have identified such an activity in HeLa nuclear extracts and are pursuing its isolation (J. Genschel and P.M., unpublished data).

The PMS2 metal binding motif $DQHA(X)_2E(X)_4E$ is required for MutLα endonuclease function and likely comprises part of the endonuclease active site. This motif is highly conserved in eukaryotic homologs of human PMS2 and MLH3 but is lacking in homologs of human MLH1 and PMS1. Interestingly, like the MLH1•PMS2 (MutLα) complex, the human MLH1•MLH3 (MutLγ) heterodimer supports mismatch repair whereas human MLH1•PMS1 (MutLβ) does not (Raschle et al., 1999; Cannavo et al., 2005). Furthermore, we have found that yeast

MutSα, MutLα, RFC, and PCNA support endonucleolytic incision of nicked heteroduplex DNA in a manner similar to the human proteins and that yeast MutLα displays weak endonuclease in the presence of ATP•Mn^{2+} (F.A.K., S. Holmes, M. Arana, T. Kunkel, and P.M., unpublished data). The $DQHA(X)_2E(X)_4E$ motif is also present in archaeal and eubacterial MutL proteins but is absent in MutL proteins from bacteria like *E. coli* that rely on d(GATC) methylation to direct mismatch repair (Figure 5E). In contrast to the heteroduplex endonuclease activity supported by human and yeast proteins, we have been unable to detect a similar activity using near homogeneous preparations of *E. coli* MutS, MutL, the β replication clamp, and the γ complex clamp loader, in either the presence or absence of SSB and DNA helicase II (O. Lukianova, M. O'Donnell, and P.M., unpublished data). These system differences might suggest a role for the $DQHA(X)_2E(X)_4E$ endonuclease motif in strand discrimination; however, as noted above, mismatch-dependent activation of MutLα endonuclease is restricted to preincised heteroduplexes. The absence of this MutL motif in systems that rely on d(GATC) methylation for strand discrimination may therefore reflect fundamental differences in the modes of excision initiation in these different organisms, an idea that is supported experimentally (Dao and Modrich, 1998; Dzantiev et al., 2004).

In addition to its role in postreplication mismatch repair, MutLα has been implicated in the cellular response to certain types of DNA damage (Stojic et al., 2004), as well as meiotic and mitotic recombination phenomena (Surtees et al., 2004). While we tend to view the strand-specific reactions described here and elsewhere (Genschel and Modrich, 2003; Dzantiev et al., 2004; Constantin et al., 2005; Zhang et al., 2005) in the context of postreplication repair, it would not be surprising if the MutLα endonucleolytic function were to contribute to these other pathways as well.

EXPERIMENTAL PROCEDURES

Proteins

Construction of expression vectors for MutLαD699N and MutLαE705K is described in the Supplemental Data. Human RFC (85%–90% pure; Figure S5); recombinant human MutSα, MutLα, MutLαD699N, MutLαE705K, ExoIb, PCNA, and RPA; and yeast RFCΔN (all ≥95% pure) were isolated as described (Dzantiev et al., 2004). Recombinant yeast RFC (95% pure) was purified according to Finkelstein et al. (2003). Other than ExoI, all proteins were free of detectable exonucleolytic activity (Dzantiev et al., 2004; Table S2). Protein concentrations were determined using the Bio-Rad Protein Assay Kit with bovine serum albumin (BSA, Pierce) as standard and are expressed as moles of heterodimer for MutSα and MutLα, moles of monomer for ExoIb, moles of heterotrimer for RPA, moles of homotrimer for PCNA, and moles of heteropentamer for both human and yeast RFC.

Mismatch-Provoked DNA Hydrolytic and Repair Reactions

Construction of heteroduplex substrates is described in the Supplemental Data. Mismatch-provoked hydrolytic reactions were performed by a minor modification of the previously described method (Dzantiev et al., 2004). Unless indicated otherwise, reactions (40 μl) contained 20 mM HEPES-KOH (pH 7.6), 125 mM KCl, 5 mM $MgCl_2$, 2 mM ATP, 1 mM dithiothreitol (DTT), 1 mM glutathione, 0.5 mg/ml bovine serum albumin (BSA), 5% (vol/vol) glycerol, and 0.2 μg substrate DNA (1.2 nM nicked 5′ or 3′ DNA or 1 nM gapped 3′ DNA). MutSα (25 nM), MutLα (20 nM), RFC (9 nM), PCNA (30 nM), RPA (100 nM), ExoIb (2.5 nM), or 100 μg human nuclear extract was present as indicated. BSA was omitted from reactions containing nuclear extract. Repair of gapped 3′ heteroduplex in 100 μg nuclear extract was determined under the buffer conditions described above, but reactions also contained 0.2 mM each dATP, dGTP, dCTP, and dTTP and were supplemented with MutLα as indicated.

After incubation at 37°C for 10 min, reactions were terminated as described previously (Dzantiev et al., 2004) or by the addition 30 μl of 0.35% SDS, 0.3 mg/ml Proteinase K, 0.4 M NaCl, 0.3 mg/ml glycogen, 5 mM $MgCl_2$, followed by incubation of the samples at 55°C for 15 min. After extraction with phenol/chloroform and isopropanol precipitation, recovered DNA was digested with NheI and ClaI (or HindIII and AlwNI for the gapped 3′ heteroduplex) to score excision (Genschel et al., 2002; Dzantiev et al., 2004) or BspEI and AlwNI to score mismatch repair of the gapped 3′ heteroduplex. Alternatively, DNA products were hydrolyzed with the indicated restriction enzyme, resolved by electrophoresis through alkaline 0.9%–1% agarose, transferred to a nylon membrane, and probed with the indicated ^{32}P-labeled oligonucleotide (Fang and Modrich, 1993; Dzantiev et al., 2004). To reprobe a membrane with a different oligonucleotide, the membrane was stripped by incubation in two changes (15–20 min each) of 0.2 M NaOH, one change of water, and one change of 0.1 M Tris-acetate (pH 7.4), 0.1% SDS with rotation. Hybridized probe was visualized and quantitated using a Molecular Dynamics PhosphorImager.

ATP•Mn^{2+}-Dependent Endonuclease Assays

Mn^{2+}-dependent endonuclease activity on covalently closed circular DNA was determined in 40 μl reactions containing 20 mM HEPES-KOH (pH 7.6), 23 mM KCl, 1 mM $MnSO_4$, 0.5 mM ATP as indicated, 1 mM DTT, 1 mM glutathione, 0.5 mg/ml BSA, 2% (vol/vol) glycerol, and 0.2 μg (1.2 nM) supercoiled f1MR59 (Dzantiev et al., 2004) or G-T heteroduplex DNA. MutSα (25 nM), MutLα (20 nM or as indicated), PCNA (30 nM), and RFC (9 nM) were included as indicated. Incubation was at 37°C for 20 min, and reactions were terminated by addition of SDS, EDTA, and Proteinase K to 0.1%, 14 mM, and 0.1 mg/ml, respectively. After further incubation at 55°C for 15 min, PMSF was added to 4 mM, and products were resolved by electrophoresis through 0.8% agarose in 40 mM Tris-acetate, 1 mM EDTA (pH 8.2). After staining with 0.5 μg/ml ethidium bromide, DNA species were quantified using a cooled photometric grade CCD camera and ImageJ software.

Fe^{2+}-Induced Protein Cleavage

EDTA was removed from wild-type and mutant MutLα preparations by dialysis against 800–1000 volumes of 50 mM HEPES-KOH (pH 7.4), 10% (wt/vol) glycerol, 0.2 M NaCl, 2 mM DTT, 1 μg/ml aprotinin, 1 μg/ml leupeptin, 1 μg/ml E64, and 0.7 μg/ml pepstatin. Dialyzed samples (0.1–0.35 μM MutLα) were incubated on ice in 50 μl reactions containing 50 mM HEPES-KOH (pH 7.4), 1% glycerol, 20 mM NaCl, 2 mM DTT in the absence or presence of 20 μM $FeCl_2$ for 15–16 hr (Zaychikov et al., 1996). Reactions were stopped by addition of EDTA to 5.7 mM, and protein products were resolved by electrophoresis through 12% or 4%–12% polyacrylamide gels in the presence of 0.1% SDS. After transfer to PVDF membranes (GE Healthcare), proteins were visualized by Western analysis using α-PMS2 antibodies directed against PMS2 residues 9–54 (Novus) or residues 800–862 (Santa Cruz Biotechnologies) or α-MLH1 antibodies against the full-length protein (Calbiochem) or MLH1 residues 633–662 (Novus). Immune complexes were detected with horseradish-peroxidase-conjugated secondary antibodies and the ECL Plus system (GE Healthcare).

Supplemental Data

Supplemental Data include Supplemental Experimental Procedures, Supplemental References, seven figures, and two tables and can be

found with this article online at http://www.cell.com/cgi/content/full/126/2/297/DC1/.

ACKNOWLEDGMENTS

We are grateful to Josef Jiricny for provision of baculovirus constructs for expression of His-tagged wild-type and ATPase-deficient forms of MutLα. We thank Vickers Burdett for construction of M13mp18/B276 and M13mp18/N276 used for preparation of gapped heteroduplex substrates, Elisabeth Penland for growth of cell lines, and Celia Baitinger for assistance with Biacore experiments. This work was supported in part by NIH grant GM45190. P.M. is an Investigator of the Howard Hughes Medical Institute.

Received: October 25, 2005
Revised: March 20, 2006
Accepted: May 15, 2006
Published: July 27, 2006

REFERENCES

Ash, D.E., and Schramm, V.L. (1982). Determination of free and bound manganese(II) in hepatocytes from fed and fasted rats. J. Biol. Chem. *257*, 9261–9264.

Au, K.G., Welsh, K., and Modrich, P. (1992). Initiation of methyl-directed mismatch repair. J. Biol. Chem. *267*, 12142–12148.

Blackwell, L.J., Wang, S., and Modrich, P. (2001). DNA chain length dependence of formation and dynamics of hMutSα•hMutLα• heteroduplex complexes. J. Biol. Chem. *276*, 33233–33240.

Bowers, J., Tran, P.T., Joshi, A., Liskay, R.M., and Alani, E. (2001). MSH-MLH complexes formed at a DNA mismatch are disrupted by the PCNA sliding clamp. J. Mol. Biol. *306*, 957–968.

Cannavo, E., Marra, G., Sabates-Bellver, J., Menigatti, M., Lipkin, S.M., Fischer, F., Cejka, P., and Jiricny, J. (2005). Expression of the MutL homologue hMLH3 in human cells and its role in DNA mismatch repair. Cancer Res. *65*, 10759–10766.

Constantin, N., Dzantiev, L., Kadyrov, F.A., and Modrich, P. (2005). Human mismatch repair: Reconstitution of a nick-directed bidirectional reaction. J. Biol. Chem. *280*, 39752–39761.

Dao, V., and Modrich, P. (1998). Mismatch, MutS, MutL, and helicase II-dependent unwinding from the single-strand break of an incised heteroduplex. J. Biol. Chem. *273*, 9202–9207.

Dzantiev, L., Constantin, N., Genschel, J., Iyer, R.R., Burgers, P.M., and Modrich, P. (2004). A defined human system that supports bidirectional mismatch-provoked excision. Mol. Cell *15*, 31–41.

Fang, W.-h., and Modrich, P. (1993). Human strand-specific mismatch repair occurs by a bidirectional mechanism similar to that of the bacterial reaction. J. Biol. Chem. *268*, 11838–11844.

Finkelstein, J., Antony, E., Hingorani, M.M., and O'Donnell, M. (2003). Overproduction and analysis of eukaryotic multiprotein complexes in *Escherichia coli* using a dual-vector strategy. Anal. Biochem. *319*, 78–87.

Galburt, E.A., and Stoddard, B.L. (2002). Catalytic mechanisms of restriction and homing endonucleases. Biochemistry *41*, 13851–13860.

Genschel, J., and Modrich, P. (2003). Mechanism of 5′-directed excision in human mismatch repair. Mol. Cell *12*, 1077–1086.

Genschel, J., Bazemore, L.R., and Modrich, P. (2002). Human exonuclease I is required for 5′ and 3′ mismatch repair. J. Biol. Chem. *277*, 13302–13311.

Grachev, M.A., Lukhtanov, E.A., Mustaev, A.A., Zaychikov, E.F., Abdukayumov, M.N., Rabinov, I.V., Richter, V.I., Skoblov, Y.S., and Chistyakov, P.G. (1989). Studies of the functional topography of *Escherichia coli* RNA polymerase. A method for localization of the sites of affinity labelling. Eur. J. Biochem. *180*, 577–585.

Gu, L., Hong, Y., McCulloch, S., Watanabe, H., and Li, G.M. (1998). ATP-dependent interaction of human mismatch repair proteins and dual role of PCNA in mismatch repair. Nucleic Acids Res. *26*, 1173–1178.

Guo, S., Presnell, S.R., Yuan, F., Zhang, Y., Gu, L., and Li, G.M. (2004). Differential PCNA requirement in 5′ and 3′ nick-directed excision in human mismatch repair. J. Biol. Chem. *279*, 16912–16917.

Habraken, Y., Sung, P., Prakash, L., and Prakash, S. (1998). ATP-dependent assembly of a ternary complex consisting of a DNA mismatch and the yeast MSH2–MSH6 and MLH1–PMS1 protein complexes. J. Biol. Chem. *273*, 9837–9841.

Iyer, R.R., Pluciennik, A., Burdett, V., and Modrich, P. (2006). DNA mismatch repair: functions and mechanisms. Chem. Rev. *106*, 302–323.

Kunkel, T.A., and Erie, D.A. (2005). DNA mismatch repair. Annu. Rev. Biochem. *74*, 681–710.

Lee, B., Nguyen, L.H., Barsky, D., Fernandes, M., and Wilson, D.M., 3rd. (2002). Molecular interactions of human Exo1 with DNA. Nucleic Acids Res. *30*, 942–949.

Lee, S.D., and Alani, E. (2006). Analysis of interactions between mismatch repair initiation factors and the replication processivity factor PCNA. J. Mol. Biol. *355*, 175–184.

Li, G.-M., and Modrich, P. (1995). Restoration of mismatch repair to nuclear extracts of H6 colorectal tumor cells by a heterodimer of human MutL homologs. Proc. Natl. Acad. Sci. USA *92*, 1950–1954.

Miyaki, M., Nishio, J., Konishi, M., Kikuchi-Yanoshita, R., Tanaka, K., Muraoka, M., Nagato, M., Chong, J.M., Koike, M., Terada, T., et al. (1997). Drastic genetic instability of tumors and normal tissues in Turcot syndrome. Oncogene *15*, 2877–2881.

Peltomaki, P. (2005). Lynch syndrome genes. Fam. Cancer *4*, 227–232.

Prolla, T.A., Pang, Q., Alani, E., Kolodner, R.D., and Liskay, R.M. (1994). MLH1, PMS1, and MSH2 interactions during the initiation of DNA mismatch repair in yeast. Science *265*, 1091–1093.

Raschle, M., Marra, G., Nystrom-Lahti, M., Schar, P., and Jiricny, J. (1999). Identification of hMutLβ, a heterodimer of hMLH1 and hPMS1. J. Biol. Chem. *274*, 32368–32375.

Raschle, M., Dufner, P., Marra, G., and Jiricny, J. (2002). Mutations within the hMLH1 and hPMS2 subunits of the human MutLalpha mismatch repair factor affect its ATPase activity, but not its ability to interact with hMutSalpha. J. Biol. Chem. *277*, 21810–21820.

Stojic, L., Brun, R., and Jiricny, J. (2004). Mismatch repair and DNA damage signalling. DNA Repair (Amst.) *3*, 1091–1101.

Su, S.-S., Lahue, R.S., Au, K.G., and Modrich, P. (1988). Mispair specificity of methyl-directed DNA mismatch correction in vitro. J. Biol. Chem. *263*, 6829–6835.

Surtees, J.A., Argueso, J.L., and Alani, E. (2004). Mismatch repair proteins: key regulators of genetic recombination. Cytogenet. Genome Res. *107*, 146–159.

Tomer, G., Buermeyer, A.B., Nguyen, M.M., and Liskay, R.M. (2002). Contribution of human *mlh1* and *pms2* ATPase activities to DNA mismatch repair. J. Biol. Chem. *277*, 21801–21809.

Wei, K., Clark, A.B., Wong, E., Kane, M.F., Mazur, D.J., Parris, T., Kolas, N.K., Russell, R., Hou, H., Jr., Kneitz, B., et al. (2003). Inactivation of Exonuclease 1 in mice results in DNA mismatch repair defects, increased cancer susceptibility, and male and female sterility. Genes Dev. *17*, 603–614.

Zaychikov, E., Martin, E., Denissova, L., Kozlov, M., Markovtsov, V., Kashlev, M., Heumann, H., Nikiforov, V., Goldfarb, A., and Mustaev, A. (1996). Mapping of catalytic residues in the RNA polymerase active center. Science *273*, 107–109.

Zhang, Y., Yuan, F., Presnell, S.R., Tian, K., Gao, Y., Tomkinson, A.E., Gu, L., and Li, G.M. (2005). Reconstitution of 5′-directed human mismatch repair in a purified system. Cell *122*, 693–705.